

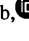




Carbon nanoscroll-based memory cell

Andrei I. Siahlo^{a, }, Sergey A. Vyrko^{a, }, Andrey M. Popov^{b, }, Nikolai A. Poklonski^{a, ,*},
Yurii E. Lozovik^{b, c, }

^a Physics Department, Belarusian State University, Nezavisimosti Ave. 4, Minsk, 220030, Belarus

^b Institute of Spectroscopy of Russian Academy of Sciences, Fizicheskaya Str. 5, Troitsk, Moscow, 108840, Russia

^c Moscow Institute of Electronics and Mathematics, National Research University Higher School of Economics, Bol. Trekhsvjatitel'skij per., 1-3/12, build. 8, Moscow, 101000, Russia

ARTICLE INFO

Dataset link: [10.17632/sm9xmywk58](https://doi.org/10.17632/sm9xmywk58)

Keywords:

Carbon nanoscroll
Memory cell
Nanorelay
NEMS
Archival memory

ABSTRACT

The scheme and operational principles of the nanoelectromechanical memory cells are proposed. These cells, which use two electrodes and a third gate electrode, operate by electrostatic unrolling of a carbon nanoscroll due to an applied voltage. Memory cell operation relies on two stable states: nonconducting Off state (rolled nanoscroll) and conducting On state (partially or fully unrolled nanoscroll). Based on the analysis of the memory cell energetics, the switching voltage between Off and On states is calculated as a function of the cell dimensions. The lower limit of the switching voltage is estimated to be about 5 V for two electrode cells and 15 V for cells with a third gate electrode. For cell dimensions that result in full nanoscroll unrolling in the On state, a return to the Off state is impossible. These cells are promising for archival memory applications, and the optimal cell dimensions for such applications are determined.

1. Introduction

Carbon nanoobjects such as graphene and nanotubes have excellent electronic and elastic properties and simultaneously are chemically inert and stable at high temperature that makes them to be promising for application in various nanoelectromechanical systems (NEMS). Particularly a wide set of nanoelectromechanical switches and memory cells based on graphene and carbon nanotubes have been produced [1–13] and considered theoretically [14–32] (see also Refs. [33–35] for a review).

Carbon nanoscrolls, yet another carbon nanoobjects, have been produced in two recent decades by various methods of synthesis: chemical vapor deposition [36–38], ball milling of graphite [39], electrochemical graphite exfoliation [40–42], microexplosion method [43,44], electrostatic deposition of graphene layers [45], rolling of a graphene layer on a substrate immersed into solution [46], rolling around nanowires [47] and around water nanodroplet [48], and use of microwave sparks in liquid nitrogen [49].

Here a scheme and principles of operation of nanoelectromechanical memory cells with two electrodes and the third gate electrode which are based on unrolling of carbon nanoscroll are proposed and the switching voltage of these memory cells is calculated as a function of sizes of the

memory cell parts. The sizes of the memory cell parts for such memory cells usable in archival memory are calculated. The small switching time (related with small Q-factor) in comparison with memory cells based on graphene and carbon nanotubes is discussed.

2. Concept of memory cell

The possibility of NEMSs based on carbon nanoobjects to operate as memory cells is based on the following properties of these nanoobjects. First, the easiness of relative motion or bending of carbon nanotube walls and graphene layers allows to design bistable systems with the existence of two minima of potential energy of the system as a function of relative positions of its movable parts with the possibility of switching between states corresponding to these minima (so called bistability). Second, the high conductivity of carbon nanotube walls and graphene layers allows to design the systems with considerably different conductance of the system in the states corresponding to these minima that allows to use these states as the nonconducting Off state and the conducting On state of the memory cell. Moreover the high conductivity allows to use electrostatic force to control motion of movable parts of the memory cell. Thus the set of memory cells and switches where movable carbon nanoobjects are used for switch-

* Corresponding author.

E-mail addresses: popov-isan@mail.ru (A.M. Popov), poklonski@bsu.by (N.A. Poklonski).

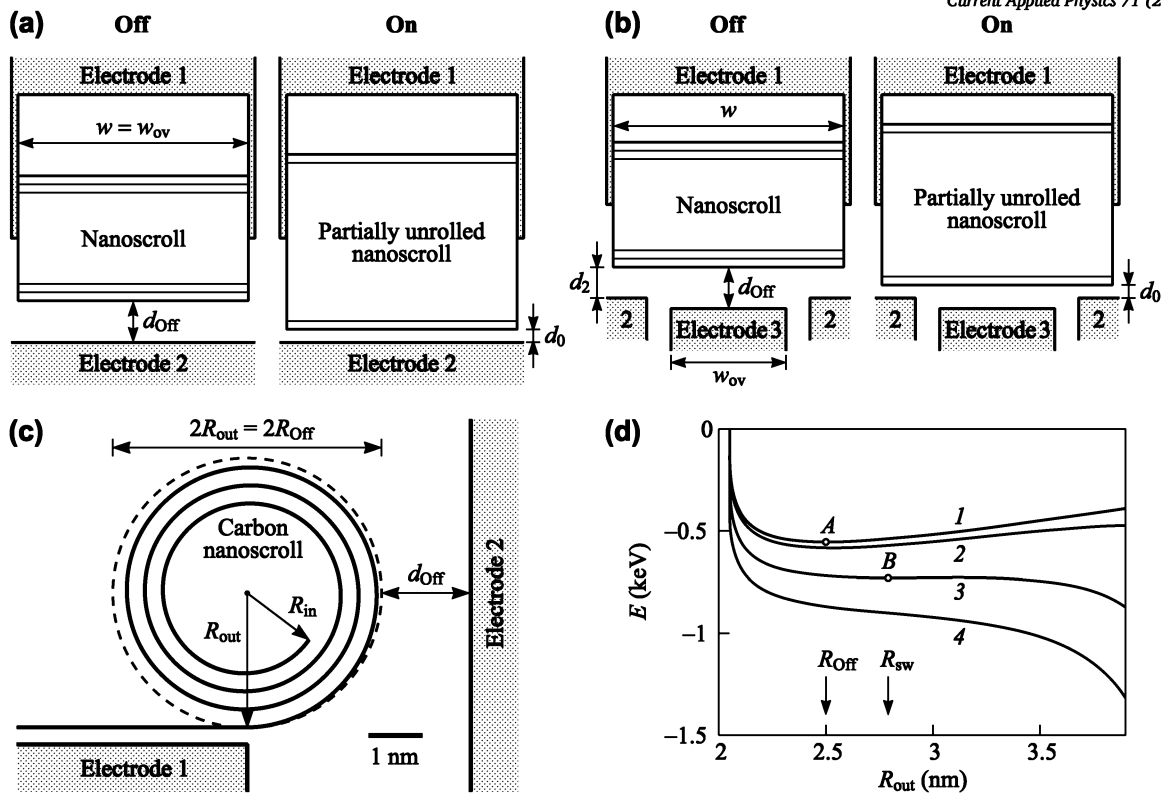


Fig. 1. Schemes of the nanoscroll-based memory cells with two electrodes (a) and the third gate electrode (b) in the Off and On states (top view). Here w is the nanoscroll length along its axis, w_{ov} is the overlap length between the nanoscroll and electrode 2 or electrode 3 for the memory cells with two and three electrodes, respectively, d_0 is the equilibrium distance of van der Waals interaction between the nanoscroll and the plane of electrode 2 (when the partially unrolled nanoscroll sticks to electrode 2), d_{off} is the distance between the nanoscroll and the plane of control electrode (electrode 2 and electrode 3 for the memory cells with two electrodes and the third gate electrode, respectively) in the Off state, $d_2 < d_{off}$ is the distance between the nanoscroll and the plane of electrode 2 for the memory cell with the third gate electrode. (c) Cross-section (side view) of the nanoscroll-based memory cell with two electrodes in the Off state with the nanoscroll outer radius $R_{out} = R_{off} = 2.5$ nm, the nanoscroll inner radius $R_{in} = 1.444$ nm, the distance $d = d_{off} = 1.68$ nm between the nanoscroll and electrode 2, and the length $L = 39$ nm across the nanoscroll axis of the initial rectangular graphene layer used to produce the nanoscroll. Cross-section of the cylinder used in calculations of the memory cell capacitance is shown by the dashed line. (d) Energy of the memory cell E as a function of the nanoscroll outer radius R_{out} calculated by Eq. (1) for the memory cell with the sizes in the Off state corresponding to panel (c) and the nanoscroll length along its axis $w = 20$ nm (and equal to the overlap length w_{ov}) at the different applied voltages between the electrodes 1 and 2: 0 V (curve 1), 3 V (2), the switching voltage $U_{sw} = 7.2$ V (3), and 10 V (4). Point A on curve 1 corresponds to the first minimum and maximum in the dependence $E(R_{out})$ at the applied switching voltage U_{sw} .

ing the conductance between electrodes are implemented and considered [1–5,7–21,24,28,30,31]. Namely, such memory cells are based on relative motion of carbon nanotube walls [5,7,19,20] and graphene layers [24], bending of carbon nanotubes [1–4,12,14–18,21], a graphene membrane [8–10,13,28,30,31], and a graphene cantilever [9,31]. The schemes of memory cells with three electrodes where the third gate electrode used for switching between Off and On states have been also considered [2–4,11,12,15–17,20,30,31]. Such a scheme allows to separate the electrical circuits used for recording and reading of the state of the memory cell. By analogy we consider schemes of the memory cells based on unrolling of a carbon nanoscroll with two and three electrodes shown in Figs. 1a and 1b, respectively. For the memory cell in the non-conducting state Off a rolled carbon nanoscroll is attached to electrode 1, and the conducting state On a partially or totally unrolled nanoscroll is attached to both electrode 1 and electrode 2.

A considerable advance has been made in the last decades in the development of the information carriers with increasing reading and recording rates and density of information. However such advance leads to more and more new types of information carriers and therefore to necessity of information rerecording. Moreover the typical lifetime of modern information carriers is 10–30 years [50]. Because of this, the development of new information carriers for an archival memory with a lifetime of hundreds of years is a pressing problem.

An archival memory needs materials which are stable against chemical, mechanical and thermal treatment and request a high lifetime of spontaneous switching between the On and Off states. Since carbon nanomaterials are highly stable and chemically inert two types of archival memory cells based on such nanomaterials have been proposed: the memory cell based on the motion of a magnetic iron nanoparticle inside a carbon nanotube [51] and the memory cell based on bending of a graphene membrane [28]. Both these memory cells have a huge energetic barrier between the On and Off states which excludes the spontaneous switching between these states due to thermodynamical fluctuations at heating. However the memory cell based on the motion of a magnetic nanoparticle requires the probe with a magnetic tip for recording and reading of information. As for the memory cell based on a graphene membrane, the switching from the On state with a bent membrane to the Off state with a flat membrane is possible at mechanical treatment on the archival memory. Here we propose the On state of the archival memory cell based on carbon nanoscroll which corresponds to a fully unrolled nanoscroll into a graphene layer, so that reverse rolling of the graphene layer into the nanoscroll corresponding to the Off state is highly unlikely at any treatment. According to calculations the carbon nanoscroll lifetime for unrolling into flat graphene nanoribbon due to thermodynamical fluctuations at room temperature exceeds 1000 years for any reasonable sizes of the nanoscroll [52]. This means that sponta-

neous switching of the memory cell from the state Off to the state On is also highly unlikely.

Below we consider the memory cell operation and perform calculations of its operational characteristics for the memory cell with two electrodes. Then the applicability of the calculated characteristics for the memory cell with three electrodes is discussed in Section 4.3.

3. Energetics of memory cell

Let us consider the energetics of the nanoscroll-based memory cell which related with calculations of the switching voltage. The total energy E of the memory cell is given by

$$E = E_{\text{ns}} + E_C, \quad (1)$$

where E_{ns} is the total energy of a carbon nanoscroll and E_C is the electrostatic energy of the memory cell. As it is discussed below in Section 4.2 the energy E_{W2} of van der Waals interaction between the nanoscroll and the plane of electrode 2 can be disregarded at the calculations of the switching voltage.

According to [52], the total energy E_{ns} of a carbon nanoscroll rolled up from a rectangular graphene layer of sizes w (in direction of the nanoscroll axis) and L in the form of an Archimedean spiral ($R = h\varphi/2\pi$) with a distance h between adjacent turns is the sum of the energy of van der Waals interaction between adjacent layers in the nanoscroll E_W and elastic bending energy of the nanoscroll E_{el} :

$$\begin{aligned} E_{\text{ns}} &= E_W + E_{\text{el}}; \\ E_W &= \frac{1}{2} \frac{\varepsilon w L_{\text{ov}}}{S_a} = \frac{1}{2} \frac{\varepsilon w}{S_a} [L(\varphi_{\text{in}}, \varphi_{\text{out}} - 2\pi) + L(\varphi_{\text{in}} + 2\pi, \varphi_{\text{out}})], \\ E_{\text{el}} &= \frac{2\pi C w}{h S_a} \int_{\varphi_{\text{in}}}^{\varphi_{\text{out}}} \frac{\sqrt{1 + \varphi^2}}{\varphi^2} d\varphi = \\ &= \frac{2\pi C w}{h S_a} \left[\frac{\sqrt{1 + \varphi_{\text{in}}^2}}{\varphi_{\text{in}}} - \frac{\sqrt{1 + \varphi_{\text{out}}^2}}{\varphi_{\text{out}}} + \right. \\ &\quad \left. + \ln(\varphi_{\text{out}} + \sqrt{1 + \varphi_{\text{out}}^2}) - \ln(\varphi_{\text{in}} + \sqrt{1 + \varphi_{\text{in}}^2}) \right], \end{aligned} \quad (2)$$

where $\varepsilon < 0$ is the energy of interaction between graphite layers per carbon atom, $C = 20.1 \text{ meV} \cdot \text{nm}^2/\text{atom}$ is the elastic constant for graphene layer bending obtained by density functional theory based calculations [52], $h = 0.3354 \text{ nm}$ is the distance between graphite layers, $S_a = 3\sqrt{3}a_{\text{CC}}^2/4 = 0.0262 \text{ nm}^2$ is the area per carbon atom in graphene, $a_{\text{CC}} = 0.142 \text{ nm}$ is the distance between carbon atoms, L_{ov} is the total length of the adjacent layers overlap for the nanoscroll cross-section, $L(\varphi_{\text{in}}, \varphi_{\text{out}})$ is the length of the Archimedean spiral with the inner angle $\varphi_{\text{in}} = 2\pi R_{\text{in}}/h$ and the outer angle $\varphi_{\text{out}} = 2\pi R_{\text{out}}/h$, where R_{in} and R_{out} are the inner and outer radii of the nanoscroll, respectively (see Fig. 1c);

$$\begin{aligned} L(\varphi_{\text{in}}, \varphi_{\text{out}}) &= \int_{\varphi_{\text{in}}}^{\varphi_{\text{out}}} \frac{h}{2\pi} \sqrt{1 + \varphi^2} d\varphi = \\ &= \frac{h}{4\pi} \left[\varphi_{\text{out}} \sqrt{1 + \varphi_{\text{out}}^2} - \varphi_{\text{in}} \sqrt{1 + \varphi_{\text{in}}^2} + \right. \\ &\quad \left. + \ln(\varphi_{\text{out}} + \sqrt{1 + \varphi_{\text{out}}^2}) - \ln(\varphi_{\text{in}} + \sqrt{1 + \varphi_{\text{in}}^2}) \right]. \end{aligned} \quad (3)$$

The nanoscroll is in the ground state for the state Off of the memory cell. Note that the ground state internal structure of the nanoscroll is uniquely determined by the single geometrical parameter [52]. That is the inner radius R_{in} , the size L of the rectangular graphene layer, the total length L_{ov} of the adjacent layers overlap, and the number of layers of the nanoscroll at the state Off of the memory cell are determined by

the outer radius R_{Off} of the nanoscroll at the state Off. We use here the outer radius R_{Off} as a convenient parameter that determines the operational characteristics of the memory cell, since this radius can be easily measured before memory cell fabrication.

Diverse experimental studies give the following data for the interlayer interaction energy ε in graphite: $-52 \pm 5 \text{ meV/atom}$ [53], $-43 \pm 5 \text{ meV/atom}$ [54], $-35_{-10}^{+15} \text{ meV/atom}$ [55] and $-31 \pm 2 \text{ meV/atom}$ [56]. We use the average value $\varepsilon = -35 \text{ meV/atom}$ with correction corresponding to interaction between incommensurate graphene layers, that is the only case possible for stacking of adjacent layers of a carbon nanoscroll, see details in Ref. [52]. Note that the scatter of the values of the interlayer interaction energy in diverse experiments determines the accuracy of our calculations of operational characteristics of the nanoscroll based memory cell to be about 50%, that allows to use below a rather crude model for the memory cell geometry and energy which disregards edge effects.

When a voltage U is applied between electrodes 1 and 2 the nanoscroll and the plane of electrode 2 acquire charges Q of the opposite sign and equal in magnitude. The electrostatic energy of the “nanoscroll + plane of electrode 2” system [57] is

$$E_C = -\frac{Q^2}{2C_{\text{cell}}} = -\frac{1}{2} C_{\text{cell}} U^2, \quad (4)$$

where C_{cell} is the memory cell capacitance, i.e., the capacitance of the “nanoscroll + plane of electrode” system.

The capacitance C_{cell} of the “nanoscroll + plane” system is calculated as the capacitance of the system consisting of an infinite plane and an infinite cylinder of radius R_{out} , the axis of which is parallel to the plane, coincides with the axis of nanoscroll and located at a distance $R_{\text{out}} + d$ from the plane [58]

$$C_{\text{cell}} = \frac{2\pi\varepsilon_0 w_{\text{ov}}}{\ln[(R_{\text{out}} + d + \sqrt{2R_{\text{out}}d + d^2})/R_{\text{out}}]}, \quad (5)$$

where ε_0 is the electric constant, w_{ov} is the length of the overlap between the nanoscroll and electrode 2 (the cross-section of the cylinder is shown in Fig. 1c by the dashed line). Eq. (5) is adequate if $R_{\text{out}} \ll w_{\text{ov}}$. The carbon nanoscrolls produced by various methods have high aspect ratio, $R_{\text{out}} \ll w$ [36–41, 43–49]. Thus the condition $R_{\text{out}} \ll w_{\text{ov}}$ can be easily fulfilled. The analogous macroscopic approach to calculate the electrostatic energy is widely used at calculation of operational characteristics of NEMSs based on carbon nanotubes [5, 14–18, 20] and a graphene membrane [28]. Such a macroscopic approach is also consistent with the above-mentioned accuracy of calculations within the framework of our model of the memory cell.

4. Calculated characteristics of memory cell

4.1. Sizes of archival memory cell

The length L_{ov} of the adjacent layers overlap decreases at unrolling of the nanoscroll under the action of the electrostatic force which occurs with increase of the outer radius R_{out} . Evidently that there is some critical value R_c of the outer radius where the length L_{ov} of the overlap becomes zero that is the nanoscroll does not exist for $R_{\text{out}} > R_c$. This means that for the memory cell with the distance d_{Off} between the nanoscroll surface and the electrode 2 in the Off state which is greater than $d_c = R_c - R_{\text{Off}} + d_0$, where d_0 is the equilibrium distance of van der Waals interaction between the nanoscroll and electrode 2, the nanoscroll does not exist in the On state and becomes a bent graphene layer which cannot roll up back into the nanoscroll, that is the Off state becomes impossible. The memory cells with values of the distance $d_{\text{Off}} > d_c$ are proposed above for usage in an archival memory. The memory cell in the On state with the distance $d_{\text{Off}} = d_c$ corresponding to the critical value R_c of the outer radius is shown in Fig. 2b.

The maximum possible distance d_{Off} for the archival memory cell cannot achieve the length L of the graphene layer which arises after full

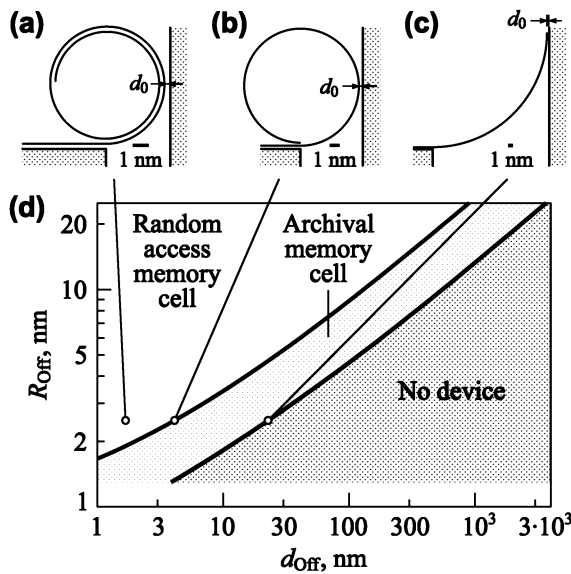


Fig. 2. (a)–(c) Cross-sections of the nanoscroll based memory cells with two electrodes in the On state with the same outer radius $R_{\text{off}} = 2.5$ nm of the nanoscroll in the Off state and the different distances $d_{\text{off}} = 1.68$ nm (a), $d_{\text{off}} = 4.11$ nm (b), and $d_{\text{off}} = 22.73$ nm (c) from the nanoscroll to the plane of electrode 2 in the Off state. (d) Diagram of the sizes of the memory cell in the Off state, R_{off} and d_{off} , where the memory cell can be used in an archival memory (filled with light yellow color) and operation of the memory cell is not possible (filled with light blue color). The sizes corresponding to the memory cells shown in panels (a), (b) and (c) are labeled by open red circles. (For interpretation of the colors in the figure, the reader is referred to the web version of this article.)

unrolling of the nanoscroll since a good contact between this graphene layer and the electrode 2 is necessary in the On state. A good contact is possible in a case where the ground state structure of the graphene layer in the On state includes a some part which is parallel to the surface of the second electrode due to van der Waals attraction. However for the distances d_{off} that are somewhat less than the length L the graphene layer can attach the second electrode only by the edge. The minimum elastic bending energy of the graphene layer with parallel edges corresponds to the shape which is a part of a cylinder. Such a shape is possible with decreasing the distances d_{off} at the fixed length L until the radius of this cylinder is greater than $R_{\text{off}} + d_{\text{off}}$. With further decreasing the distance d_{off} one part of the graphene layer has a shape which is close to a quarter of a cylinder with radius $R_{\text{off}} + d_{\text{off}}$ and other is attracted to the surface of the second electrode providing a good contact. Thus we roughly estimate the maximum possible distance d_{off} as corresponding to the case where the bent graphene layer forms a quarter of a cylinder, see Fig. 2c. Note that accurate estimations with account of the energy of van der Waals interaction between the graphene layer and the second electrode should give a somewhat greater value of the maximum possible distance d_{off} . The calculated sizes of the memory cell in the Off state (R_{off} and d_{off}) which corresponds to usage in an archival memory are shown in Fig. 2d.

4.2. Switching voltage

To calculate the switching voltage from the Off state to the On state let us first consider what occurs with an increase of the voltage U applied between the electrodes 1 and 2. The dependences of the total energy E of the memory cell on the nanoscroll outer radius R_{out} calculated by Eq. (1) for the different voltages U are shown in Fig. 1d. When a small voltage U is applied, the nanoscroll is attracted to the electrode 2 by the electrostatic force with slight unrolling of the nanoscroll so that position of the first minimum in the dependence $E(R_{\text{out}})$ is shifted from the value R_{off} in the Off state corresponding to the ground

state of the nanoscroll (shown by point A in Fig. 1d) to greater value and the barrier between the Off and On states of the memory cell somewhat decreases due to contribution of the electrostatic energy. With further increase of the voltage U the barrier between the Off and On states disappears, therefore the Off state corresponding to the rolled nanoscroll becomes unstable and the nanoscroll is attached to the electrode 2 with abrupt partial or full unrolling so that the switching of the memory cell to the conducting On state takes place. The voltage U where this barrier disappears is the switching voltage U_{sw} of the memory cell. The disappearance of the barrier between Off and On states means that the first minimum and the maximum in the dependence $E(R_{\text{out}})$ coincide at some value R_{sw} of the nanoscroll outer radius, $R_{\text{out}} = R_{\text{sw}}$ (shown by point B in Fig. 1d). It is easy to show that the switching voltage is the same for the memory cells with the same ratio w_{ov}/w of the overlap length between the electrode 2 and the nanoscroll to the nanoscroll length. The switching voltage U_{sw} is calculated here by analysis of the numerical solution of equation

$$\frac{dE(R_{\text{out}})}{dR_{\text{out}}} = F_1(R_{\text{out}}) + \frac{w_{\text{ov}}}{w} U_{\text{sw}}^2 F_2(R_{\text{out}}) = 0, \quad (6)$$

where F_1 and F_2 are functions of two memory cell sizes in the Off state: the initial distance d_{off} between the nanoscroll and the electrode 2 and the ground state outer radius R_{off} of the nanoscroll.

Let us show that the contribution of the energy E_{W2} of van der Waals interaction between the nanoscroll and the surface of electrode 2 into the energetics of the memory cell which determined the switching voltage is negligible due to the following reason. This energy E_{W2} contributes to the determination of the switching voltage U_{sw} at the switching distance d_{sw} between outer surface of the nanoscroll and the plane of electrode 2 where the minimum in the dependence $E(R_{\text{out}})$ disappears and the Off state of the memory cell becomes unstable at applying of the switching voltage U_{sw} (the distance d_{sw} corresponds to the nanoscroll outer radius R_{sw} shown by point B in Fig. 1d). First, according to random phase approximation-based calculations the equilibrium distances between the graphene layer and surfaces of various metals $d_0 < 0.4$ nm whereas the interaction energy per one atom of graphene corresponds to the range 50–90 meV/atom [59] that is close to interlayer interaction energy of graphite as it is discussed above. Simultaneously the area of possible contact between the nanoscroll and the surface of the second electrode is considerably less than the area of layer overlap within the nanoscroll at the switching distance d_{sw} . Second, energy of van der Waals interaction steeply decreases with increase of distance. Namely, this energy is proportional to $(r_0/r)^6$ for atom-atom interaction, where r and r_0 are the interatomic distance and equilibrium interatomic distance, respectively, that is the energy is proportional to $(d_0/d_a)^4$ for atom-surface interaction, where d_a is the distance between an atom and a surface. We consider here the operation of the memory cell for the sizes in the Off state (R_{off} and d_{off}) where the distance d_{sw} is at least several times greater than the equilibrium distance d_0 between the nanoscroll and the surface of electrode 2 in the On state. In this case the condition $(d_0/d_a)^4 \ll 1$ is fulfilled that is the energy of van der Waals interaction between the nanoscroll and the surface of electrode is considerably less than the energy of van der Waals interaction between layers within the nanoscroll E_W and therefore can be disregarded. Note that for the memory cell sizes in the Off state, $R_{\text{off}} = 2.5$ nm and $d_{\text{off}} = 1.68$ nm, shown in Fig. 1c the switching distance $d_{\text{sw}} = 1.4$ nm is several times greater than the equilibrium distance $d_0 < 0.4$ nm and $(d_0/d_a)^4 \approx 0.007 \ll 1$.

The minimum outer radius of the obtained nanoscrolls is about 5 nm [36] whereas the nanoscrolls with the outer radius of about 10 nm are fabricated by various methods [41–43,49]. Since it is important for a memory cell to have a minimum size (that correlates with a small switching time and a low switching voltage) we do not consider memory cells with great sizes of parts and do not determine the upper limit of the switching voltage. The calculated dependences of the switching voltage U_{sw} on the outer radius R_{off} of the nanoscroll in the Off state of the

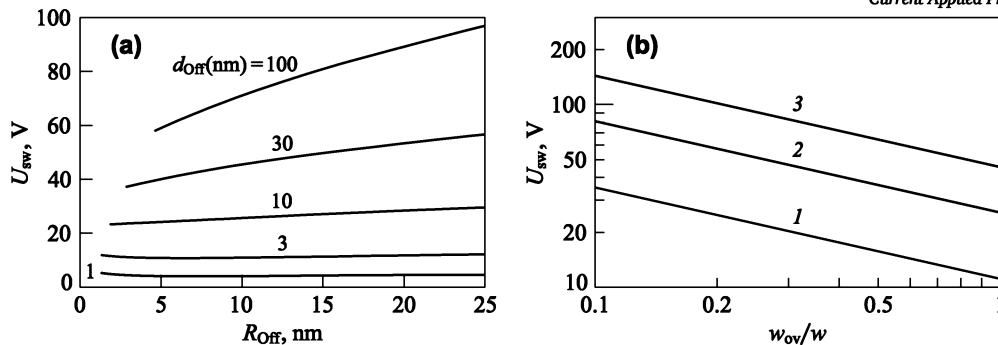


Fig. 3. Dependence of the switching voltage U_{sw} on the sizes of the parts of the nanoscroll-based memory cells with two electrodes: (a) on the outer radius R_{Off} of the nanoscroll in the Off state for the different distances $d_{Off} = 1, 3, 10, 30$, and 100 nm between the nanoscroll and the electrode 2 in the Off state and the ratio of the overlap length between the electrode 2 and the nanoscroll to the nanoscroll length $w_{ov}/w = 1$, (b) on the ratio w_{ov}/w for the memory cells with the following sizes in the Off state: $R_{Off} = 3$ nm, $d_{Off} = 3$ nm (line 1), $R_{Off} = 10$ nm, $d_{Off} = 10$ nm (line 2), $R_{Off} = 10$ nm, $d_{Off} = 30$ nm (line 3).

memory cell with the ratio $w_{ov}/w = 1$ and the different distances d_{Off} between the nanoscroll and the electrode 2 in the Off state are shown in Fig. 3a. The switching voltage only slightly depends on the outer radius R_{Off} of the nanoscroll and is determined mainly by the distance d_{Off} . For ease of operation of an electromechanical memory cell a sufficiently low switching voltage is necessary. Since it is hardly possible to fabricate the memory cell with the distance d_{Off} less than 1 nm, the lower limit of the switching voltage U_{sw} is estimated to be about 5 V. The switching voltages of the implemented nanotube-based memory cells fall within the range 5–100 V [2–5,7]. Note that the weak dependence of the switching voltage U_{sw} on the outer radius R_{Off} means that there is no necessity to separate nanoscrolls with the narrow range of the radii for batch fabrication of the memory cells with the close values of the switching voltage.

4.3. Memory cell with three electrodes

The calculated characteristics of the memory cell with two electrodes are applicable for the memory cell with three electrodes taking into account the differences between the schemes of these memory cells (see Figs. 1a and 1b). At the calculations of the memory cell sizes corresponding to archival memory (see Fig. 2) the distance d_{Off} is the distance from the nanoscroll to the plane of electrode 2 in the Off state both for the memory cells with two and three electrodes. However at the calculations of the switching voltage the distance d_{Off} for the memory cell with three electrodes is the distance from the nanoscroll to the plane of gate electrode 3 in the Off state. The length w_{ov} for the memory cell with three electrodes is the length of the overlap between the nanoscroll and the electrode 3. It is evident from Eq. (6) that for the memory cell with the different fixed sizes R_{Off} and d_{Off} the switching voltage U_{sw} depends on the ratio w_{ov}/w of the overlap length between the electrode and the nanoscroll to the nanoscroll length as follows: $U_{sw}(w_{ov}/w) = U_{sw}(1)/\sqrt{w_{ov}/w}$, where $U_{sw}(1)$ is the switching voltage for the memory cell with $w_{ov}/w = 1$. The calculated dependences $U_{sw}(w_{ov}/w)$ for several memory cells with the fixed sizes R_{Off} and d_{Off} are shown in Fig. 3b.

Let us estimate the lower limit of the switching voltage U_{sw} for the memory cell with three electrodes. There are two differences in schemes of the memory cell with two and three electrodes which both lead to increase of this lower limit. First, the minimal possible distance d_2 between outer surface of the nanoscroll and the plane of electrode 2 (see Fig. 1b) for the memory cell with three electrodes is hardly to be less than 1 nm (similar to the two-electrode cell estimate). To prevent a contact in the On state between outer surface of the nanoscroll and the plane of gate electrode 3 the distance d_{Off} should exceed the distance d_2 at least by 1–2 nm. Second, it is evident that for the memory cell with three electrodes the ratio w_{ov}/w cannot range up to the maximum value equal to 1 as it can take place for the memory cell with two elec-

trodes. For the distance $d_{Off} = 3$ nm and $w_{ov}/w = 0.7$ the lower limit of the switching voltage U_{sw} is estimated to be about 15 V.

5. Conclusions

The schemes and operational principles of the memory cells with two and three electrodes based on unrolling of carbon nanoscroll by the electrostatic force caused by the applied voltage are proposed. The analysis of the energetics of the memory cell operation is used to calculate the switching voltage of between the nonconducting Off and conducting On states as a function of sizes of the memory cell parts: the nanoscroll outer radius, the distance between the nanoscroll and the electrode in the state Off, and the ratio of the overlap length between the electrode and the nanoscroll to the nanoscroll length along its axis. The lower limit of the switching voltage is estimated to be about 5 and 15 V for the memory cells with two electrodes and the third gate electrode, respectively, that is convenient for the usage. Moreover the switching voltage only slightly depends on the outer radius of the nanoscroll. Therefore batch fabrication of the nanoscroll-based memory cells with close values of the switching voltage is possible without preliminary separation of the nanoscroll with the certain radii from a nanoscroll mixture. If a full unrolling of the nanoscroll occurs in the On state, the reverse rolling of the nanoscroll and therefore existence of the Off state becomes impossible. We propose that such memory cells can be used in an archival memory. The possible sizes of the memory cells for the archival memory are calculated.

Let us also compare the proposed carbon nanoscroll-based memory cell with the carbon nanotube-based [1–5,7,14–21] and graphene-based [8,24,28] memory cells. The important characteristics of an electromechanical memory cell are the space occupied by the memory cell and the switching time. First, memory cells based on 1D carbon nanoobjects (nanotubes and nanoscrolls) can occupy less space than memory cells based on 2D graphene. Second, the switching time of an electromechanical memory cell is determined by damping of vibration of movable parts after the switching to the On state since such vibrations prevent identification of the On state [16,18]. Thus low Q-factor is desirable for vibration of the memory cell movable parts. High Q-factor has been observed for bending vibrations of a carbon nanotube, $Q \sim 40$ –500 [60,61] and for relative telescopic axial oscillations of carbon nanotube walls, $Q \sim 100$ –1000, see, e.g., Ref. [62] and references therein. However telescopic oscillations of a graphene flake on a graphene layer have very low Q-factor, $Q \sim 1$ –10, related with flexural vibrations of the flake [63]. During the unrolling of the carbon nanoscroll flexural vibrations at the rim area near the inner and outer nanoscroll edges are also possible. Therefore we believe that unrolling-rolling vibrations of the nanoscroll which can arise at the switching of the nanoscroll-based memory cell to the On state have low Q-factor and this memory cell has small switching time of the same order of magnitude as unrolling/rolling time of the

nanoscroll. The molecular dynamics simulations give the rolling time in the range 0.04–2 ns [64–67] for the small nanoscrolls consisting of 2–5 layers (that is less number of layers than in the produced nanoscrolls). Taking into account that the rolling time increases with the increase of the number of layers in the nanoscroll (or the outer radius) and Q-factor $Q \sim 1$ –10 the switching time can be estimated in the range 0.1–100 ns depending on the sizes of the memory cell parts. Thus the proposed carbon nanoscroll-based memory cell combines advantages of carbon nanotube-based and graphene-based memory cells and has both a small occupied space and a small switching time.

CRediT authorship contribution statement

Andrei I. Siahlo: Methodology, Software, Investigation. **Sergey A. Vyrko:** Investigation, Methodology, Visualization, Writing — reviewing & editing. **Andrey M. Popov:** Conceptualization, Methodology, Writing — original draft. **Nikolai A. Poklonski:** Funding acquisition, Project administration, Supervision, Writing — reviewing & editing. **Yurii E. Lozovik:** Funding acquisition, Project administration, Supervision, Writing — reviewing & editing.

Declaration of competing interest

The authors declare that they have no known competing financial interests or personal relationships that could have appeared to influence the work reported in this paper.

Acknowledgements

A.M.P. and Y.E.L. acknowledge the support by the Russian Science Foundation grant No. 23-42-10010, <https://rscf.ru/en/project/23-42-10010/>. S.A.V. and N.A.P. acknowledge support by the Belarusian Republican Foundation for Fundamental Research (Grant No. F23RNF-049) and by the Belarusian National Research Program “Convergence-2025” (Task No. 3.02.1.1).

Data availability

The raw data that support the findings of this study are openly available in *Mendeley Data* at <https://doi.org/10.17632/sm9xmywk58>, see Ref. [68].

References

- [1] T. Rueckes, K. Kim, E. Joselevich, G.Y. Tseng, C.-L. Cheung, C.M. Lieber, Carbon nanotube-based nonvolatile random access memory for molecular computing, *Science* 289 (5476) (2000) 94–97, <https://doi.org/10.1126/science.289.5476.94>.
- [2] S.W. Lee, D.S. Lee, R.E. Morjan, S.H. Jhang, M. Sveningsson, O.A. Nerushev, Y.W. Park, E.E.B. Campbell, A three-terminal carbon nanorelay, *Nano Lett.* 4 (10) (2004) 2027–2030, <https://doi.org/10.1021/nl049053v>.
- [3] S.N. Cha, J.E. Jang, Y. Choi, G.A.J. Amaratunga, D.-J. Kang, D.G. Hasko, J.E. Jung, J.M. Kim, Fabrication of a nanoelectromechanical switch using a suspended carbon nanotube, *Appl. Phys. Lett.* 86 (2005) 083105, <https://doi.org/10.1063/1.1868064>.
- [4] J.E. Jang, S.N. Cha, Y. Choi, G.A.J. Amaratunga, D.J. Kang, D.G. Hasko, J.E. Jung, J.M. Kim, Nanoelectromechanical switches with vertically aligned carbon nanotubes, *Appl. Phys. Lett.* 87 (2005) 163114, <https://doi.org/10.1063/1.2077858>.
- [5] V.V. Deshpande, H.-Y. Chiu, H.W.C. Postma, C. Mikó, L. Forró, M. Bockrath, Carbon nanotube linear bearing nanoswitches, *Nano Lett.* 6 (6) (2006) 1092–1095, <https://doi.org/10.1021/nl052513f>.
- [6] K.-T. Lam, C. Lee, G. Liang, Bilayer graphene nanoribbon nanoelectromechanical system device: a computational study, *Appl. Phys. Lett.* 95 (2009) 143107, <https://doi.org/10.1063/1.3243695>.
- [7] A. Subramanian, L.X. Dong, B.J. Nelson, A. Ferreira, Supermolecular switches based on multiwalled carbon nanotubes, *Appl. Phys. Lett.* 96 (2010) 073116, <https://doi.org/10.1063/1.3327514>.
- [8] H. Zhang, W. Bao, Z. Zhao, J.-W. Huang, B. Standley, G. Liu, F. Wang, P. Kratz, L. Jing, M. Bockrath, C.N. Lau, Visualizing electrical breakdown and ON/OFF states in electrically switchable suspended graphene break junctions, *Nano Lett.* 12 (4) (2012) 1772–1775, <https://doi.org/10.1021/nl203160x>.
- [9] J. Sun, M. Muruganathan, N. Kanetake, H. Mizuta, Locally-actuated graphene-based nano-electro-mechanical switch, *Micromachines* 7 (7) (2016) 124, <https://doi.org/10.3390/mi7070124>.
- [10] J. Sun, M.E. Schmidt, M. Muruganathan, H.M.H. Chong, H. Mizuta, Large-scale nanoelectromechanical switches based on directly deposited nanocrystalline graphene on insulating substrates, *Nanoscale* 8 (12) (2016) 6659–6665, <https://doi.org/10.1039/C6NR00253F>.
- [11] N. Huynh Van, M. Muruganathan, J. Kulothungan, H. Mizuta, Fabrication of a three-terminal graphene nanoelectromechanical switch using two-dimensional materials, *Nanoscale* 10 (26) (2018) 12349–12355, <https://doi.org/10.1039/C7NR08439K>.
- [12] S.A. Abbasi, T.-H. Kim, S. Somu, H. Wang, Z. Chai, M. Upmanyu, A. Busnaina, Fabrication of a nanoelectromechanical bistable switch using directed assembly of SWCNTs, *J. Phys. D: Appl. Phys.* 53 (23) (2020) 23LT02, <https://doi.org/10.1088/1361-6463/ab7e61>.
- [13] M.E. Chen, M.M. Rojo, F. Lian, J. Koeln, A. Sood, S.M. Bohaichuk, C.M. Neumann, S.G. Garrow, K.E. Goodson, A.G. Alleyne, E. Pop, Graphene-based electromechanical thermal switches, *2D Mater.* 8 (3) (2021) 035055, <https://doi.org/10.1088/2053-1583/abf08e>.
- [14] M. Dequesnes, S.V. Rotkin, N.R. Aluru, Calculation of pull-in voltages for carbon-nanotube-based nanoelectromechanical switches, *Nanotechnology* 13 (1) (2002) 120–131, <https://doi.org/10.1088/0957-4484/13/1/325>.
- [15] J.M. Kinaret, T. Nord, S. Viefers, A carbon-nanotube-based nanorelay, *Appl. Phys. Lett.* 82 (8) (2003) 1287–1289, <https://doi.org/10.1063/1.1557324>.
- [16] L.M. Jonsson, T. Nord, J.M. Kinaret, S. Viefers, Effects of surface forces and phonon dissipation in a three-terminal nanorelay, *J. Appl. Phys.* 96 (1) (2004) 629–635, <https://doi.org/10.1063/1.1756689>.
- [17] L.M. Jonsson, S. Axelsson, T. Nord, S. Viefers, J.M. Kinaret, High frequency properties of a CNT-based nanorelay, *Nanotechnology* 15 (11) (2004) 1497–1502, <https://doi.org/10.1088/0957-4484/15/11/022>.
- [18] J.W. Kang, O.K. Kwon, J.H. Lee, H.J. Lee, Y.-J. Song, Y.-S. Yoon, H.J. Hwang, Nanoelectromechanical carbon nanotube memory analysis, *Physica E* 33 (1) (2006) 41–49, <https://doi.org/10.1016/j.physe.2005.10.013>.
- [19] L. Maslov, Concept of nonvolatile memory based on multiwall carbon nanotubes, *Nanotechnology* 17 (10) (2006) 2475–2482, <https://doi.org/10.1088/0957-4484/17/10/007>.
- [20] A.M. Popov, E. Bichoutskaia, Yu.E. Lozovik, A.S. Kulish, Nanoelectromechanical systems based on multi-walled nanotubes: nanothermometer, nanorelay, and nanoactuator, *Phys. Status Solidi A* 204 (6) (2007) 1911–1917, <https://doi.org/10.1002/pssa.200675322>.
- [21] N.A. Poklonski, E.F. Kislyakov, S.A. Vyrko, N.N. Hieu, O.N. Bubel', A.I. Siahlo, I.V. Lebedeva, A.A. Knizhnik, A.M. Popov, Yu.E. Lozovik, Magnetically operated nanorelay based on two single-walled carbon nanotubes filled with endofullerenes Fe@C₂₀, *J. Nanophotonics* 4 (2010) 041675, <https://doi.org/10.1117/1.3417104>.
- [22] I.V. Lebedeva, A.A. Knizhnik, A.M. Popov, Yu.E. Lozovik, B.V. Potapkin, Modeling of graphene-based NEMS, *Physica E* 44 (6) (2012) 949–954, <https://doi.org/10.1016/j.physe.2011.07.018>.
- [23] S.Y. Kim, S.-Y. Cho, K.-S. Kim, J.W. Kang, Developing nanoscale inertial sensor based on graphite-flake with self-retracting motion, *Physica E* 50 (2013) 44–50, <https://doi.org/10.1016/j.physe.2013.02.025>.
- [24] A.M. Popov, I.V. Lebedeva, A.A. Knizhnik, Yu.E. Lozovik, B.V. Potapkin, Structure, energetic and tribological properties, and possible applications in nanoelectromechanical systems of argon-separated double-layer graphene, *J. Phys. Chem. C* 117 (21) (2013) 11428–11435, <https://doi.org/10.1021/jp402765p>.
- [25] H.J. Hwang, J.W. Kang, Nonvolatile graphene nanoflake shuttle memory, *Physica E* 56 (2014) 17–23, <https://doi.org/10.1016/j.physe.2013.08.009>.
- [26] J.W. Kang, J. Park, O.K. Kwon, Developing a nanoelectromechanical shuttle graphene-nanoflake device, *Physica E* 58 (2014) 88–93, <https://doi.org/10.1016/j.physe.2013.12.001>.
- [27] I.V. Lebedeva, A.M. Popov, A.A. Knizhnik, Yu.E. Lozovik, N.A. Poklonski, A.I. Siahlo, S.A. Vyrko, S.V. Ratkevich, Tunneling conductance of telescopic contacts between graphene layers with and without dielectric spacer, *Comput. Mater. Sci.* 109 (2015) 240–247, <https://doi.org/10.1016/j.commatsci.2015.07.006>.
- [28] A.I. Siahlo, A.M. Popov, N.A. Poklonski, Yu.E. Lozovik, S.A. Vyrko, S.V. Ratkevich, Multi-layer graphene membrane based memory cell, *Physica E* 84 (2016) 348–353, <https://doi.org/10.1016/j.physe.2016.08.003>.
- [29] M. Stopa, T. Rueckes, Theoretical study of SET operation in carbon nanotube memory cell, *Jpn. J. Appl. Phys.* 55 (4S) (2016) 04EE03, <https://doi.org/10.7567/JJAP.55.04EE03>.
- [30] J. Kulothungan, M. Muruganathan, H. Mizuta, 3D finite element simulation of graphene nano-electro-mechanical switches, *Micromachines* 7 (8) (2016) 143, <https://doi.org/10.3390/mi7080143>.
- [31] P.R. Mudimela, R. Chaudhary, Graphene cantilever-based digital logic gates, *J. Comput. Electron.* 20 (1) (2021) 81–87, <https://doi.org/10.1007/s10825-020-01545-y>.
- [32] Y. Chen, Z. Guo, T. Chang, Atomistic simulations of temperature-induced switchable morphology in graphene nanodrum, *Comput. Mater. Sci.* 222 (2023) 112102, <https://doi.org/10.1016/j.commatsci.2023.112102>.
- [33] E. Bichoutskaia, A.M. Popov, Yu.E. Lozovik, Nanotube-based data storage devices, *Mater. Today* 11 (6) (2008) 38–43, [https://doi.org/10.1016/S1369-7021\(08\)70120-2](https://doi.org/10.1016/S1369-7021(08)70120-2).
- [34] S.W. Lee, E.E.B. Campbell, Nanoelectromechanical devices with carbon nanotubes, *Curr. Appl. Phys.* 13 (8) (2013) 1844–1859, <https://doi.org/10.1016/j.cap.2013.02.023>.

- [35] T. Cai, Y. Fang, Y. Fang, R. Li, Y. Yu, M. Huang, Electrostatic pull-in application in flexible devices: a review, *Beilstein J. Nanotechnol.* 13 (2022) 390–403, <https://doi.org/10.3762/bjnano.13.32>.
- [36] W. Ruland, A.K. Schaper, H. Hou, A. Greiner, Multi-wall carbon nanotubes with uniform chirality: evidence for scroll structures, *Carbon* 41 (3) (2003) 423–427, [https://doi.org/10.1016/S0008-6223\(02\)00342-1](https://doi.org/10.1016/S0008-6223(02)00342-1).
- [37] A.L. Chuvilin, V.L. Kuznetsov, A.N. Obratsov, Chiral carbon nanoscrolls with a polygonal cross-section, *Carbon* 47 (13) (2009) 3099–3105, <https://doi.org/10.1016/j.carbon.2009.07.024>.
- [38] A.K. Schaper, M.S. Wang, Z. Xu, Y. Bando, D. Golberg, Comparative studies on the electrical and mechanical behavior of catalytically grown multiwalled carbon nanotubes and scrolled graphene, *Nano Lett.* 11 (8) (2011) 3295–3300, <https://doi.org/10.1021/nl201655c>.
- [39] J.L. Li, Q.S. Peng, G.Z. Bai, W. Jiang, Carbon scrolls produced by high energy ball milling of graphite, *Carbon* 43 (13) (2005) 2830–2833, <https://doi.org/10.1016/j.carbon.2005.06.007>.
- [40] L.M. Viculis, J.J. Mack, R.B. Kaner, A chemical route to carbon nanoscrolls, *Science* 299 (5611) (2003) 1361, <https://doi.org/10.1126/science.1078842>.
- [41] H. Shioyama, T. Akita, A new route to carbon nanotubes, *Carbon* 41 (1) (2003) 179–181, [https://doi.org/10.1016/S0008-6223\(02\)00278-6](https://doi.org/10.1016/S0008-6223(02)00278-6).
- [42] M.V. Savoskin, V.N. Mochalin, A.P. Yaroshenko, N.I. Lazareva, T.E. Konstantinova, I.V. Barsukov, I.G. Prokofiev, Carbon nanoscrolls produced from acceptor-type graphite intercalation compounds, *Carbon* 45 (14) (2007) 2797–2800, <https://doi.org/10.1016/j.carbon.2007.09.031>.
- [43] F. Zeng, Y. Kuang, Y. Wang, Z. Huang, C. Fu, H. Zhou, Facile preparation of high-quality graphene scrolls from graphite oxide by a microexplosion method, *Adv. Mater.* 23 (42) (2011) 4929–4932, <https://doi.org/10.1002/adma.201102798>.
- [44] F. Zeng, Y. Kuang, G. Liu, R. Liu, Z. Huang, C. Fu, H. Zhou, Supercapacitors based on high-quality graphene scrolls, *Nanoscale* 4 (13) (2012) 3997–4001, <https://doi.org/10.1039/C2NR30779K>.
- [45] A. Sidorov, D. Mudd, G. Sumanasekera, P.J. Ouseph, C.S. Jayanthi, S.-Y. Wu, Electrostatic deposition of graphene in a gaseous environment: a deterministic route for synthesizing rolled graphenes?, *Nanotechnology* 20 (2009) 055611, <https://doi.org/10.1088/0957-4484/20/5/055611>.
- [46] X. Xie, L. Ju, X. Feng, Y. Sun, R. Zhou, K. Liu, S. Fan, Q. Li, K. Jiang, Controlled fabrication of high-quality carbon nanoscrolls from monolayer graphene, *Nano Lett.* 9 (7) (2009) 2565–2570, <https://doi.org/10.1021/nl900677y>.
- [47] M. Yan, F. Wang, C. Han, X. Ma, X. Xu, Q. An, L. Xu, C. Niu, Y. Zhao, X. Tian, P. Hu, H. Wu, L. Mai, Nanowire templated semihollow bicontinuous graphene scrolls: designed construction, mechanism, and enhanced energy storage performance, *J. Am. Chem. Soc.* 135 (48) (2013) 18176–18182, <https://doi.org/10.1021/ja409027s>.
- [48] U. Mirsaidov, V.R.S.S. Mokkaapati, D. Bhattacharya, H. Andersen, M. Bosman, B. Özyilmaz, P. Matsudaira, Scrolling graphene into nanofluidic channels, *Lab Chip* 13 (15) (2013) 2874–2878, <https://doi.org/10.1039/C3LC50304F>.
- [49] J. Zheng, H. Liu, B. Wu, Y. Guo, T. Wu, G. Yu, Y. Liu, D. Zhu, Production of high-quality carbon nanoscrolls with microwave spark assistance in liquid nitrogen, *Adv. Mater.* 23 (21) (2011) 2460–2463, <https://doi.org/10.1002/adma.201004759>.
- [50] M. Cheshier, The storage lifetime of removable media, *Computer Technology Review (the Free Library)* (2003) August 1, <https://www.thefreelibrary.com/-a0109665179>.
- [51] G.E. Begtrup, W. Gannett, T.D. Yuzvinsky, V.H. Crespi, A. Zettl, Nanoscale reversible mass transport for archival memory, *Nano Lett.* 9 (5) (2009) 1835–1838, <https://doi.org/10.1021/nl803800c>.
- [52] A.I. Siahlo, N.A. Poklonski, A.V. Lebedev, I.V. Lebedeva, A.M. Popov, S.A. Vyrko, A.A. Knizhnik, Yu.E. Lozovik, Structure and energetics of carbon, hexagonal boron nitride, and carbon/hexagonal boron nitride single-layer and bilayer nanoscrolls, *Phys. Rev. Mater.* 2 (2018) 036001, <https://doi.org/10.1103/PhysRevMaterials.2.036001>.
- [53] R. Zacharia, H. Ulbricht, T. Hertel, Interlayer cohesive energy of graphite from thermal desorption of polyaromatic hydrocarbons, *Phys. Rev. B* 69 (2004) 155406, <https://doi.org/10.1103/PhysRevB.69.155406>.
- [54] L.A. Girifalco, R.A. Lad, Energy of cohesion, compressibility, and the potential energy functions of the graphite system, *J. Chem. Phys.* 25 (4) (1956) 693–697, <https://doi.org/10.1063/1.1743030>.
- [55] L.X. Benedict, N.G. Chopra, M.L. Cohen, A. Zettl, S.G. Louie, V.H. Crespi, Microscopic determination of the interlayer binding energy in graphite, *Chem. Phys. Lett.* 286 (5–6) (1998) 490–496, [https://doi.org/10.1016/S0009-2614\(97\)01466-8](https://doi.org/10.1016/S0009-2614(97)01466-8).
- [56] Z. Liu, J.Z. Liu, Y. Cheng, Z. Li, L. Wang, Q. Zheng, Interlayer binding energy of graphite: a mesoscopic determination from deformation, *Phys. Rev. B* 85 (2012) 205418, <https://doi.org/10.1103/PhysRevB.85.205418>.
- [57] D.C. Giancoli, *Physics: Principles with Applications*, Pearson, Boston, 2014.
- [58] J.-R. Riba, F. Capelli, Analysis of capacitance to ground formulas for different high-voltage electrodes, *Energies* 11 (5) (2018) 1090, <https://doi.org/10.3390/en11051090>.
- [59] T. Olsen, K.S. Thygesen, Random phase approximation applied to solids, molecules, and graphene-metal interfaces: from van der Waals to covalent bonding, *Phys. Rev. B* 87 (2013) 075111, <https://doi.org/10.1103/PhysRevB.87.075111>.
- [60] P. Poncharal, Z.L. Wang, D. Ugarte, W.A. de Heer, Electrostatic deflections and electromechanical resonances of carbon nanotubes, *Science* 283 (5407) (1999) 1513–1516, <https://doi.org/10.1126/science.283.5407.1513>.
- [61] V. Sazonova, Y. Yaish, H. Üstünel, D. Roundy, T.A. Arias, P.L. McEuen, A tunable carbon nanotube electromechanical oscillator, *Nature* 431 (7006) (2004) 284–287, <https://doi.org/10.1038/nature02905>.
- [62] I.V. Lebedeva, A.A. Knizhnik, A.M. Popov, Yu.E. Lozovik, B.V. Potapkin, Dissipation and fluctuations in nanoelectromechanical systems based on carbon nanotubes, *Nanotechnology* 20 (2009) 105202, <https://doi.org/10.1088/0957-4484/20/10/105202>.
- [63] A.M. Popov, I.V. Lebedeva, A.A. Knizhnik, Yu.E. Lozovik, B.V. Potapkin, Molecular dynamics simulation of the self-retracting motion of a graphene flake, *Phys. Rev. B* 84 (2011) 245437, <https://doi.org/10.1103/PhysRevB.84.245437>.
- [64] M.L. Pereira Jr., L.A. Ribeiro Jr., D.S. Galvão, J.M. De Sousa, Dynamical formation of graphene and graphane nanoscrolls, *Chem. Phys. Lett.* 780 (2021) 138919, <https://doi.org/10.1016/j.cplett.2021.138919>.
- [65] Z. Zhang, T. Li, Carbon nanotube initiated formation of carbon nanoscrolls, *Appl. Phys. Lett.* 97 (8) (2010) 081909, <https://doi.org/10.1063/1.3479050>.
- [66] H.Y. Song, S.F. Geng, M.R. An, X.W. Zha, Atomic simulation of the formation and mechanical behavior of carbon nanoscrolls, *J. Appl. Phys.* 113 (16) (2013) 164305, <https://doi.org/10.1063/1.4803034>.
- [67] D. Zhang, H. Yang, Formation of carbon nanoscrolls from graphene sheet: a molecular dynamics study, *J. Mol. Struct.* 1125 (2016) 282–287, <https://doi.org/10.1016/j.molstruc.2016.06.083>.
- [68] A.I. Siahlo, S.A. Vyrko, A.M. Popov, N.A. Poklonski, Yu.E. Lozovik, Data for: carbon nanoscroll-based memory cell, *Mendeley Data* (2025), <https://doi.org/10.17632/sm9xmywk58>.